

Supplementary Information for Friedman and Perrimon, “A functional genomic RNAi screen for novel regulators of RTK and ERK signaling,” 2006.

Supplementary Methods

Genome-wide RNAi Screening

The genome-wide dsRNA screening collection of the *Drosophila* RNAi Screening Center (DRSC) covering >95% of the *Drosophila* genome has been described previously³¹. This set includes 13,589 annotated (BDGP 3.2) targets and 6,831 predicted genes³². All *Drosophila* cell culture methods have been previously described³³.

As a screening cell line, we used S2R+ cells, a variant adherent S2 line³⁴. We established a stable cell line of S2R+ cells overexpressing cDNAs for the *Drosophila* ERK ortholog Rolled, tagged at its C-terminus with YFP, and *Drosophila* MEK, Dsor1, tagged at the N-terminus with CFP. These constructs were cloned into pUAST and expressed under actinGal4 control. We observed similar kinetics of ERK activation in response to stimulus (compare Sup. Figs. 1b and 2b) and similar effects of dsRNA knockdown of known RTK/ERK pathway components in this cell line compared to wild-type S2R+ cells (compare Sup. Figs. 1d and 3d). Furthermore, all secondary screens validating our primary screen results were performed in cells not expressing these constructs.

We adapted traditional immunocytochemistry techniques and previous HTS assays³⁵. Sixty-two 384-well plates pre-aliquoted with the DRSC library were seeded with 4×10^4 cells and incubated in serum-free medium for 45 minutes. Serum-containing medium was added and the cells grown for four days at 25°C. Subsequently, the medium was replaced with phosphate-buffer saline (PBS) (“baseline”) or PBS containing 25µg/mL bovine insulin (Sigma) (“Stimulated”) for ten minutes, which we previously established was the peak of insulin-stimulated ERK activation in this cell line. Prior to fixation, we measured total YFP fluorescence from the live cells using an Analyst GT plate reader (Molecular Devices) as an approximate measure of cell number for use during gene selection (see below). The cells were then fixed with 4% formaldehyde for 10 minutes and washed with PBS+0.1%Triton (PBST) twice.

Monoclonal antibodies directed towards the dually phosphorylated mammalian ERK1/2 were obtained from Cell Signaling Technologies, Inc. This antibody was raised against the identical peptide, highly conserved among metazoans, used to generate antibodies previously described to be sensitive and specific in *Drosophila* tissues and cells^{36,37}. The antibody was directly conjugated to Alexa 647 dye using the Alexa Fluor 647 Protein Labeling Kit (Molecular Probes). Following washing, the screening plates were incubated with 750ng/mL conjugated dpERK antibody in PBST supplemented with 3% bovine serum albumin at 4°C, overnight. Antibody solution was removed and the plates washed with PBST twice before reading YFP (which approximates total ERK, excluding endogenous protein) and Alexa 647 (dpERK) channels. Each time point (baseline and stimulated) was screened in duplicate, totaling over 92,000 dsRNAs.

Data Analysis

Our data analysis procedure was directed towards removing as many sources of noise as possible so that robust genomic information could be extracted from the screen. Many of these issues have been recently reviewed³⁸, some variations of which were applied here

Raw dpERK and ERK channel intensities were first background subtracted to account for autofluorescence of the plastic screening plates. dpERK values were then divided by ERK values for each channel to yield a normalized dpERK value. To correct spatial irregularities in the fluorescence measurements across individual screening plates, normalized dpERK values were corrected by dividing by a moving median of each well's column and row normalized dpERK values. Corrected, normalized dpERK values were converted to Z-scores, the relative number of standard deviations from the plate mean. We filtered the dataset for outliers by converting Z-scores to ranks for each plate, the replicates summed, and used the top and bottom rank-sums for future analysis. The replicate Z-scores for these wells were then averaged, and a cutoff of +/- 1.5 was chosen for the primary "hit list." This cutoff was chosen to include as many novel regulators as possible at this initial stage; only a small decrease in validation rate in secondary screening was observed for genes with a Z-score +/-1.5-2.0 compared to those with a Z-score +/- 2.0 and above (87% vs. 92%). This suggests that a continuum exists between strong regulators and those having no effect on the pathway, and other regulators, important under particular conditions or

contexts, may have been excluded. This hit list was further pruned for duplicate genes and for genes which appeared to have significant off-target effects (OTE). OTE predictions were based on our observation of a trend in amplicons of correlated lethality and increasing number of predicted 21nt overlaps with other genes (not shown). In general, 19-21nt homology with other genes appear to be a major source of false positives in previous *Drosophila* dsRNA screens³⁹. Based on this trend, we removed all genes with >10 21nt OT and >35nt maximum OT length. Since this original curation, the annotation of the *Drosophila* genome has changed and may have altered OT number; however, our filtering nevertheless removed those amplicons most likely to be false-positives. In total, 1,644 amplicons are represented in the pruned primary hit list. The complete primary screen gene list and amplicon sequences are available in Sup. Table 1 and at the DRSC website³³. Isolation of 476 predicted genes³² suggests that these may be valid transcripts, and that genome-wide functional analyses such as these can be used to validate gene predictions. Indeed, 11% of these genes scored in recent *Drosophila* gene tiling experiments⁴⁰. We found predicted genes at a slightly lower frequency than the DRSC collection overall ($p < 0.042$ by hypergeometric distribution).

We annotated our hit list for molecular function, conservation, and other features by cross-referencing publicly-available databases. GO terms were downloaded from FlyBase⁴¹, and subgroups as displayed in the text were manually curated from these specific terms; conflicts were resolved on a case-by-case basis. “Receptors” subgroup includes many classes of GO-labeled “receptors,” including RTKs. Conservation was determined using the HomoloGene⁴² and InParanoid⁴³ databases of orthologous groups; since a systematic, rather than *de novo* or hand curation was used, there may be orthologs known from specific experimental work that are not listed in our tables, and vice-versa. Human disease relevance was extracted using the Ensembl database⁴⁴ and from the Homophila database cross-referencing the *Drosophila* genome with the NCBI Online Mendelian Inheritance in Man (OMIM) project⁴⁵; an $E < 1 \times 10^{-10}$ cutoff was used for this reference.

Enrichment p values for GO term categories provided in Sup. Table 2 was performed using the hypergeometric test function implemented by the GeneNotes software previously published⁴⁶. Enrichment for pathway components and particular conservation patterns represented in Sup. Fig. 2 was similarly performed using the hypergeometric distribution. For both, the DRSC collection, not the *Drosophila* genome, was used as the background population,

in order to account for collection bias, although our library is > 95% complete. Median absolute value Z-scores for all hits at baseline (1.9, $n=651$) were compared to those of those hits at baseline conserved in humans (2.0, $n=408$) and in humans, mice, worms, and yeast (2.1, $n=200$), and p values calculated from the raw Z-score cumulative distributions using the Kolmogorov-Smirnov test. Genes conserved across all four species examined had a more significant effect on ERK signaling at baseline ($p < 0.001$) than isolated genes overall. This result implies that the core, conserved signaling cascade is modulated by proteins recently added to the regulatory network with more moderate individual effects on signal propagation. We detected no significant enrichment for genes in our primary hit list based on chromosomal location. Median Z-score of hits with particular GO term categories was compared to all hits at baseline or under stimulation (Fig. 2c) and p values calculated using the Mann-Whitney U test, FDR corrected for multiple hypotheses.

Hierarchical clustering was performed in the Cluster program using Pearson correlation or Euclidean distance, and displayed using TreeView.

Secondary Screening

The 362 genes were chosen for secondary screening/validation by selecting for particular annotation categories with known involvement in the RTK/ERK pathway, such as kinases and phosphatases; pruning all but representative members of entire molecular machines (e.g., catalytic and regulatory proteasome components, ribosomal proteins, etc.), since components of a single complex likely influence pathway activity similarly; selection for conserved components and genes with possible human disease relevance; and pruning the predicted genes³² to 10% of our list (from 29%), since only a small percentage of these have been validated by experimental data. We estimated cell number using our total ERK-YFP pre-fixation fluorescence value and biased against genes with large effects on viability, as *bona fide* pathway components did not affect this value.

dsRNA targeting these genes were resynthesized and 250ng aliquoted randomly in quintuplicate in 384-well plates along with luciferase dsRNA negative controls. In order to use wild-type cells, we modified our screening assay to use total ERK rabbit antibody (Cell Signaling), along with unconjugated dpERK mouse primary antibody. Similar plate

manipulations were used as in the primary screen, with the addition of secondary antibody and DAPI incubations. DAPI, total ERK (Alexa 488) and dpERK (Alexa 647) channels were recorded on the plate reader. Similar data analysis/normalization procedures were used as above. Normalized, corrected dpERK values are represented as percent of controls, and *p* values were calculated for each gene and assay using the Student's *t*-test. These 362 genes were screened in this format in triplicate (S2R+ baseline and insulin stimulus) or duplicate (all other conditions), and the results of the replicates combined, yielding seven assay points and corresponding *p* values for each gene. Multiple hypothesis correction (370 genes x 7 assays) was applied using the False Discovery Rate (FDR) criteria ($q < 0.05$), as previously described^{47, 48}. The FDR-corrected *p* values were used to identify hits in secondary screens which significantly affect dpERK levels in any of the given conditions. Directly comparing replicates of the same amplicons performed in parallel secondary screens resulted in validation by FDR criteria of 80-90% of the genes. Of 362 genes tested, 91% (331) had a significant effect on RTK/ERK signaling under one or more stimuli, indicating a low false-positive rate due to assay noise in the primary screen.

As stated in the text, we performed a separate series of experiments to test the contribution of “off-target effects,” e.g., knockdown of non-targeted genes due to homology^{39, 49}. We reasoned that non-overlapping amplicons targeting the same gene likely have non-overlapping OTE. Although we could not design additional amplicons for some genes, for many of our hits (~300) we designed one or two amplicons in addition to those used in the DRSC collection, and screened these in parallel to the original amplicon at baseline and under insulin stimulus in S2R+ cells. 85% of the tested genes could be validated with at least one additional amplicon. As this validation rate is equivalent to the validation rate between tests of the same amplicon, we conclude that OTE are not a significant contribution to noise in our assay. Importantly, we believe this high validation rate is a result of our pre-filtering of our primary hit list for genes with >10 21nt predicted off-targets. We have indicated the genes which validated through this assay in Sup. Table 4; other genes either did not validate (also marked) or, more often, were not tested in these additional amplicon experiments.

We used wild-type S2R+ and Kc167 cells for secondary screening of these amplicons at baseline and under insulin stimulus. Kc167 cells have a transcriptional profile distinct from the S2 cell line⁵⁰. We detected similar maximal dpERK elevation in Kc cells at 10 minutes following

insulin stimulation (Sup. Fig. 3a). For analysis under additional RTK stimuli, two stable cell lines were created (S2R+ and Kc167) which express the *Drosophila* EGF receptor, type II (DER) under the metallothionein promoter, similar to a S2 line previously described⁵¹, maintained in puromycin or hygromycin, respectively. No DER was detectable by Western blotting in wild-type S2R+ and Kc cells and no robust dpERK elevation was detected following sSpi stimulus. We observed weak but detectable DER expression by Western blotting without copper stimulus in both stable cell lines (Sup. Fig. 3b-c); this level of DER did not elevate dpERK levels compared to wild-type cells through autoactivation, but still led to DER-dependent dpERK elevation following Spitz stimulation (Sup. Fig. 3b-c). As we observed in the screening cell line, wild-type S2R+ cells stimulated with insulin and S2R+DER cells stimulated with conditioned media collected from cells expressing secreted Spitz (sSpi)⁵¹ demonstrated similar, predicted effects of knockdown of known ERK components (Sup. Fig. 3d and e, respectively). As the primary source of baseline ERK activation is through PVR⁵², genes isolated from our screen at baseline but not under insulin stimulus may be specific effectors of PVR but not InR activity (Sup. Fig. 2a). In order to extend these observations, we also screened our secondary gene list in S2R+ cells under hyper-stimulation of PVR. For PVR hyper-stimulation, we unexpectedly observed an increase in dpERK in S2R+ cells following application of serum-free medium conditioned from growth in Kc cells, compared to serum-free medium alone (Sup. Fig. 3f). This increase was reduced by knockdown of *Pvf1* and/or *Pvf2* in the Kc cells and *PVR* in the S2R+ cells, suggesting PVR hyper-stimulation, although other stimuli may also be present.

S2 cells expressing Ras^{V12} under the control of a metallothionein promoter inducible with heavy metals was kindly provided by M. Therrien⁵³. Secondary screening was performed in this cell line as before in S2R+ cells. For Ras^{V12} induction, the cells were incubated in 700 μ M CuSO₄ following three days of RNAi, and the cells fixed after 24 hours induction. Ras^{V12} was not induced before insulin stimulation in these cells. For *Gap1* epistasis, S2R+ cells were exposed to either *luciferase* or *Gap1* dsRNA and grown for two days in flasks. Each population was then plated in secondary screening plates as before. *Luciferase* dsRNA pre-incubated cells were stimulated with insulin and compared to unstimulated *Gap1* dsRNA pre-incubated cells. We found a ~30% increase in baseline dpERK levels in the *Gap1*-treated cells. Several epistatic relationships between known components and *Gap1* were not recapitulated in this data set, unlike the Ras^{V12} data; we believe this is due to the hypomorphic nature of the *Gap1* and other

gene depletions, or the strength of the hit itself, rather than the true hierarchy in the pathway. Nevertheless, many positive regulators were clearly suppressed by *Gap1* dsRNA, including 55 of the 85 genes which suppress Ras^{V12}-mediated ERK activation. Further investigation is required for genes which suppress *Gap1*- but not Ras^{V12}-mediated ERK activation.

Constructs, Immunoprecipitation and Western Blotting

Full-length cDNA clones for ERK (*Rl*), MEK (*Dsor1*), *CG5169/dGCKIII*, *CG12169/dPPM1*, and PP2A (*Mts*) were obtained from the Berkeley Drosophila Genome Project (BDGP) clone collections⁵⁴ (RE08694, LD41207, RE38276, AT28366, and LD26077, respectively); Raf (*Phl*) was a gift of L. Kockel. cDNAs were cloned using PCR (Phusion polymerase, New England Biolabs) with appropriate C-terminal tags on 3' primers (HA or Myc, as indicated) and transferred to pUAST expression vector. For ERK-YFP and CFP-MEK, cDNA for ERK and EYFP (Clontech) or MEK and ECFP (Clontech) were PCR cloned with appropriate linkers into pUAST. Mutation of dGCKIII and dPPM1 was performed using the Site-directed Mutagenesis Kit (Stratagene). Similar mutations as dGCKIII K42R was previously shown to be kinase dead in the Mst3^{55, 56} and Mst4^{57, 58} mammalian orthologs. The dPPM1 D228A mutation in a conserved metal ion binding site was previously shown inactive the mammalian⁵⁹ and yeast⁶⁰ orthologs. Stable RNAi hairpin transgenics *in vivo* were created using the DRSC amplicon for each gene cloned in a 3'-5', 5'-3' orientation using the pWiz vector⁶¹. We failed to identify significant effects of expression of a dPPM1 transgenic RNAi hairpin. All constructs were sequence verified.

For co-immunoprecipitation and Western blotting, indicated constructs were transfected with actinGal4 for constitutive expression using Effectene into 3-4 x 10⁶ S2R+ or Kc cells in 6-well dishes. After 3-4 days, cells were lysed in RIPA buffer and Western blotting performed essentially as described³⁶. Total protein levels were quantified using the BCA Protein Assay Kit (Pierce). For RNAi experiments in 6-well dishes, we used 25µg per well and scaled all other reagents similarly from 384-well plates. Primers for *dPPM1* alternate amplicon are 5' GGCCCTTCCCGCGCCCTC 3' and 5' AAGATTAGCCTCGGGAGTTTCGCTTTCGCGAAG 3'; partial overlap with the DRSC amplicon was necessary due to the small size of this gene. Primers for the *dGCKIII* alternate

amplicon are 5' CACAAGCCAGTCGAGAGCCAG 3' and 5' CAGCTTGCGCTCCGAGTGCAG 3'. Amplicon sequences for other dsRNAs are available from the DRSC.

For cell culture immunofluorescence, cells were fixed in 4% formaldehyde for 10 minutes, washed in PBS+0.1%Triton, and incubated overnight in PBST+3%BSA at 4°C with rat anti-HA (Roche). Samples were subsequently washed in PBST, incubated in fluorescently-conjugated secondary antibodies and DAPI for 1-2hr at room temperature, washed, and mounted for imaging on a Leica TCS SP2 AOBS confocal microscope.

Co-immunoprecipitation was performed according to standard protocols using agarose-conjugated monoclonal anti-Myc antibodies (Santa Cruz Biotechnology, Inc.). The following primary antibodies were used: rabbit polyclonal total ERK (Cell Signaling Technology), monoclonal mouse dpERK (Cell Signaling technology), Rat anti-HA (Roche Applied Science), rabbit anti-Myc (Santa Cruz Biotechnology), rabbit anti-DER (gift of E. Bach), rat anti-Spitz (gift of E. Bach), and guinea pig anti-PVR (gift of K. Brückner). Western blotting detection was performed using HRP-conjugated secondary antibodies (Fig. 1a and Sup. Fig. 1b) or fluorescently-conjugated secondary antibodies (Molecular Probes Alexa 680 and Rockland IRDye 800CW) and the Li-Cor Biosciences Aeries imaging system for digital, quantitative, two-channel Western blotting detection. Quantitation was performed by analyzing the integrated signal intensities for the indicated detected bands using the Li-Cor software.

Genetics

Standard *Drosophila* culture and genetic procedures were used, and all stocks except where noted are available through public stock centers or by request. We generated dGCKIII^{PWiz}, UAS-dPPM1-HA, dPPM1^{PWiz}, UAS-dPPM1-HA D228A, UAS-dGCKIII-HA, and UAS-dGCKIII K42R transgenic flies through traditional transformation techniques in the *w*¹¹¹⁸ background. The deficiency uncovering *CG5169/dGCKIII*, *w*¹¹¹⁸; *Df(3R)Exel6176*, *P{w[+mC]=XP-U}Exel6176 / TM6B*, *Tb*¹, is predicted to disrupt approximately twenty-one genes in this region⁴¹; none of the twenty other genes appeared as hits in our genome-wide screen. *y*, *w*; *apterousGal4*, *UAS-mCD8-GFP / CyO* was a gift of C. Micchelli. Other lines discussed in the text include *Elp*^{B1} / *CyO* and *FRT*^{2A}, *Gap1*^{B2} / *TM3*, *ftz-lacZ*.

For imaginal disc immunofluorescence, wing discs from third instar larvae were dissected in cold PBS, fixed for 20 minutes in 4% formaldehyde, and washed in PBS+0.1%Triton. Staining was performed overnight in PBST+3% BSA at 4°C. Discs were washed in PBST and incubated with secondary antibodies for 1-2hr at room temperature. They were subsequently washed, and mounted for imaging on a Leica TCS SP2 AOBS confocal microscope. Primary antibodies used were rabbit anti-phospho HistoneH3 (Upstate Biotechnology), rabbit anti-activated Caspase3 (Cell Signaling), and mouse anti-dpERK (Cell Signaling).

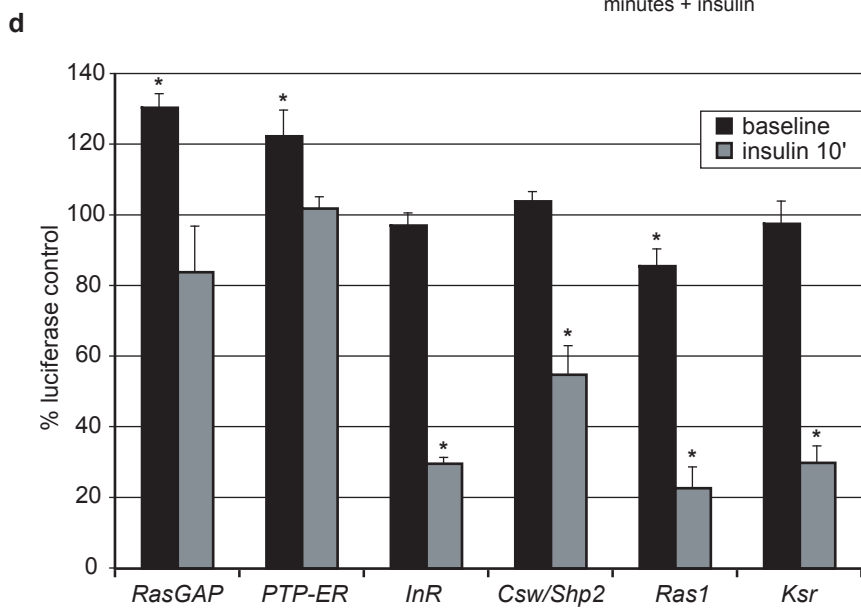
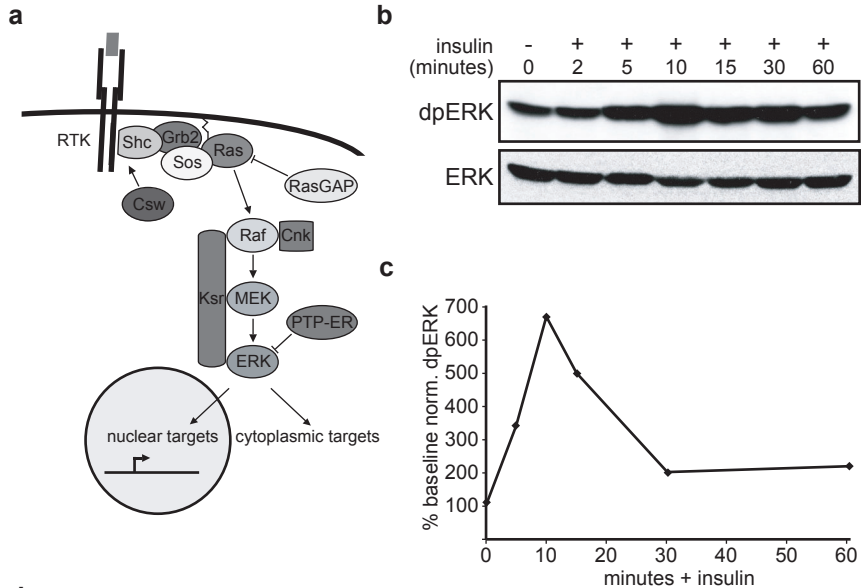
Wings of the indicated genotype were mounted in a 1:1 mixture of Permount (Fisher Scientific) and xylenes (C. Micchelli, unpublished) and imaged using a Zeiss Axioskop2 motplus. Scanning electron microscope imaging of fly eyes was performed according to standard protocols. *In situ* hybridizations of *dGCKIII* in wing discs was performed according to standard protocols.

Mammalian Cell Culture, RNAi, and RT-PCR

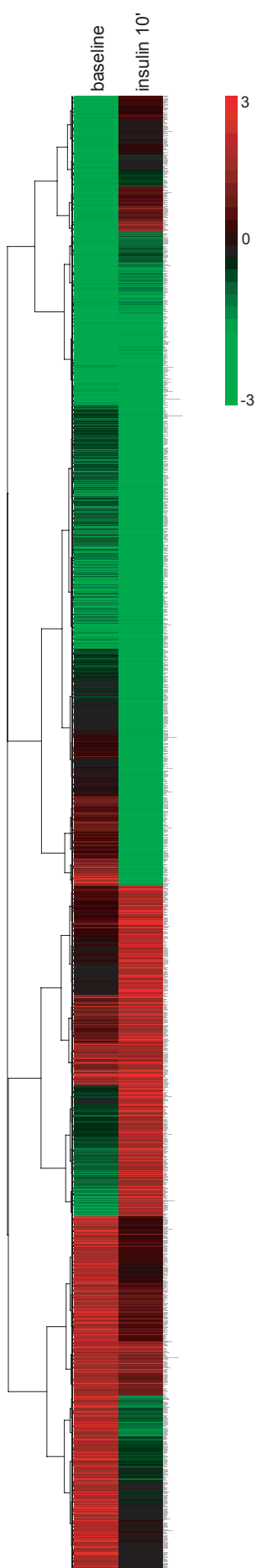
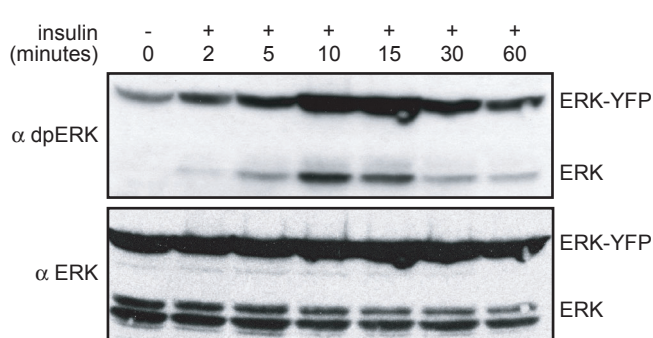
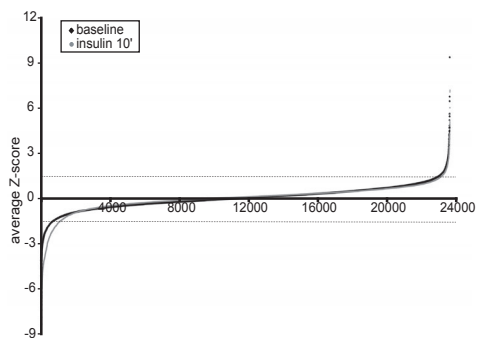
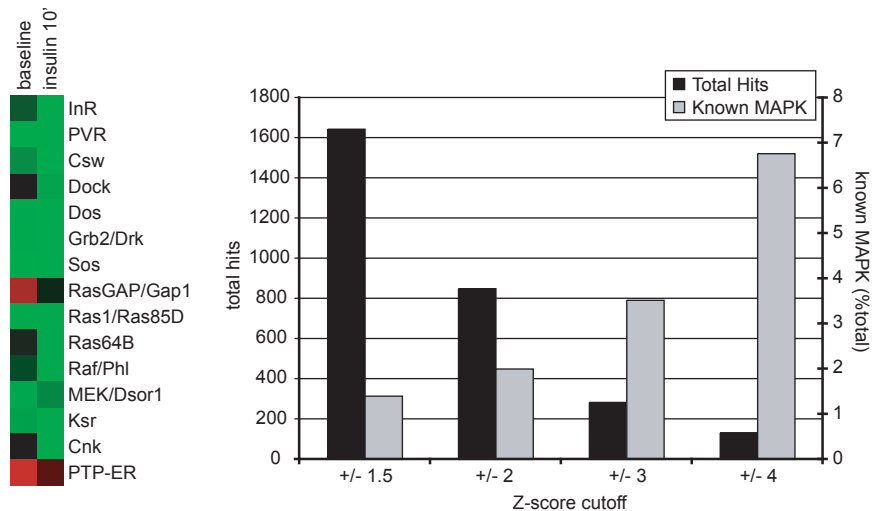
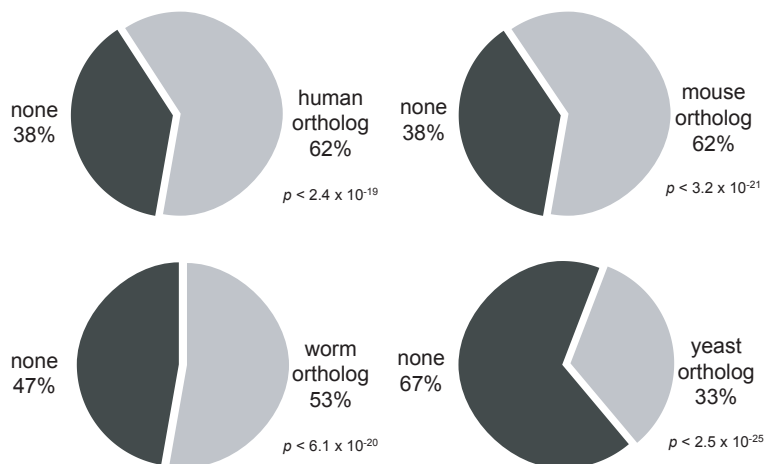
DU145 and LNCaP prostate cancer cell lines were a gift of M. Freeman and maintained in DMEM+10%FBS or RPMI+10%FBS, respectively. *Raf-1*, *Mst4/MASK*, and *Ppm1 α* siRNAs were produced from PCR products obtained from the RZPD esiRNA library and processed into dsRNA-free siRNAs using the Dicer eXtreme gene kit (Roche); we designed and processed similarly *Mst3/STK24* dsRNA targeting comparable regions as *Mst4* using the following primers: 5' TGAATTCTGTGACCAGTGATTG 3' and 5' TTCAGACATTTTTAGGTGGGAAA 3'. siRNAs were transfected into cell lines at the indicated concentration using HiPerfect transfection reagent (Qiagen). After 72 hours, overnight-starved cells were lysed or stimulated with 100ng/mL EGF (Calbiochem) and lysed in RIPA buffer. Following total protein quantitation, Western blotting to dpERK and ERK were performed as described for *Drosophila* cells.

For analysis of efficiency of siRNA knockdown, we extracted total RNA from cells 72 hours after transfection using Trizol (Invitrogen), followed by phenol:chloroform extraction and purification on RNeasy columns (Qiagen). Reverse transcription was performed using random decamer-primed AMV reverse transcriptase (Promega). PCR primers were designed spanning introns, although we did not observe any product in control reactions performed from samples

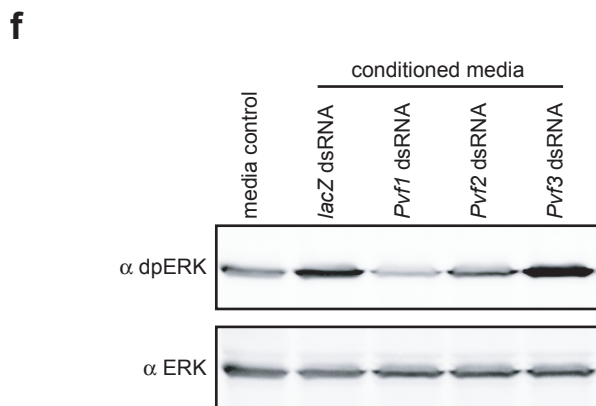
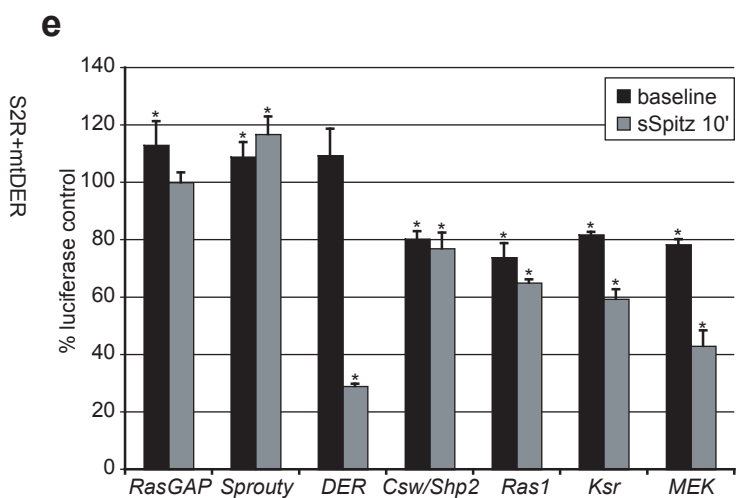
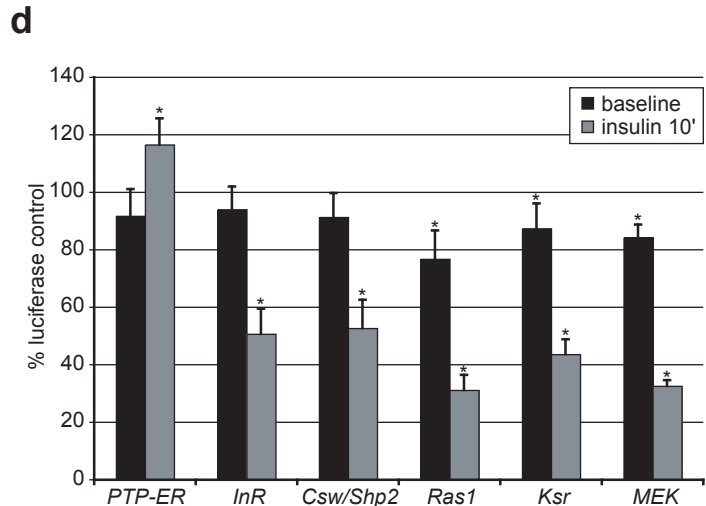
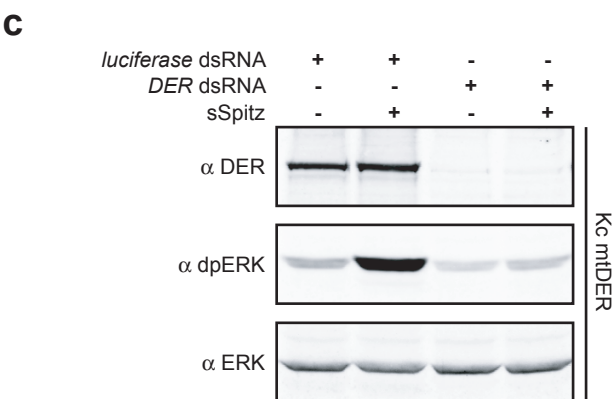
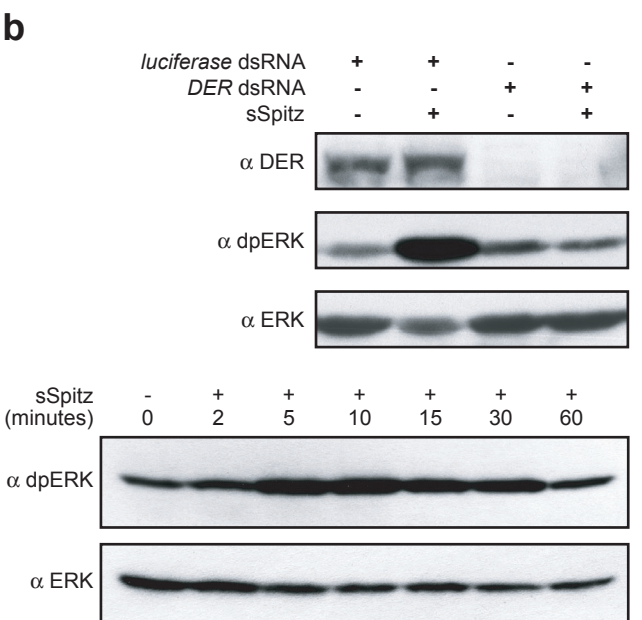
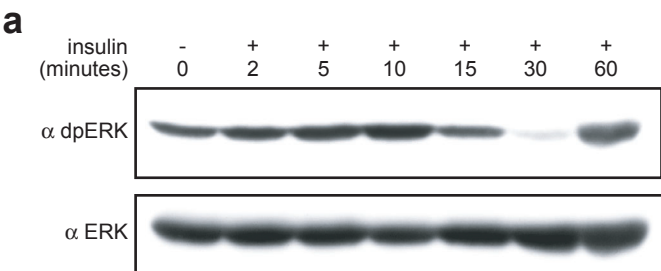
prepared without reverse transcriptase. All amplifications were within the linear range for each primer pair as determined by testing of multiple cycle numbers. Primers used were as follows: *β-actin* 5' GGCATCCTCACCCCTGAAGTA 3' and 5' AGGGCATACCCCTCGTAGAT 3', *GAPDH* 5' GAAGGTGAAGGTCGGAGTCA 3' and 5' TTCACACCCATGACGAACAT 3', *Raf-1* 5' ACAAAGGACAACCTGGCAAT 3' and 5' CCCCCGTCATCAGTTCATAC 3', *Mst3* 5' AACTTGGGGTCCATTGAAGA 3' and 5' AAAATGATCGCTGGAAGGAG 3', and *Mst4* 5' CTTGTGCAAACCCTGAGTTG 3' and 5' TGATAAACGCCATCACAAAA 3'.



Supplementary Figure 1 | High-throughput RTK/ERK screening assay. a, RTK/ERK signaling pathway in *Drosophila*. Ligand binding to RTKs induces intracellular tyrosine phosphorylation and recruitment of Src-homology-2 (SH2)-containing adaptors such as Grb2 and the Ras guanine exchange factor (GEF) Sos, activating the small GTPase Ras by GTP exchange. Ras activation results in the membrane recruitment and activation of Raf, which in turn phosphorylates MEK, which finally activates ERK1/2 through dual phosphorylation of a TEY motif within an activation loop⁶². This core signaling cassette is additionally regulated by the phosphatase corkscrew/Shp2, the scaffolds Ksr and Cnk, and negative regulators such as those of the Sprouty family, Ras GTPase activating proteins (RasGAPs), and MAPK phosphatases such as PTP-ER. Although the most well-studied effectors of ERKs are transcription factors such as the ETS family members, a wide range of nuclear and cytoplasmic targets of ERK have been documented, including components of translational control machinery and other kinases such as the ribosomal S6 kinases (RSKs) and MSKs, which in turn have a variety of downstream targets^{63, 64}. **b,** Insulin induces elevation of dpERK in wild-type S2R+ cells by Western blotting, with maximal activation at 10 minutes. **c,** Screening cell line and dpERK assay in 384-well plate format demonstrates similar activation kinetics as in **b**. dpERK values are normalized to total ERK (YFP) fluorescence. Hemocytes expressing ERK-YFP displayed identical kinetics of ERK activation and sensitivity to knockdown of known pathway components as wild-type S2R+ cells (see Methods and Sup. Fig. 2b and 3d); subsequent secondary screens were all conducted in wild-type cells. **d,** RNAi of known pathway components (negative regulators *RasGAP/Gap1* and *PTP-ER*, and positive regulators *InR*, *Csw*, *Ras1*, and *Ksr*) in screening format results in expected effects on normalized dpERK values, expressed as percent of a luciferase dsRNA negative control. * $p < 0.05$ by Student's *t* test.

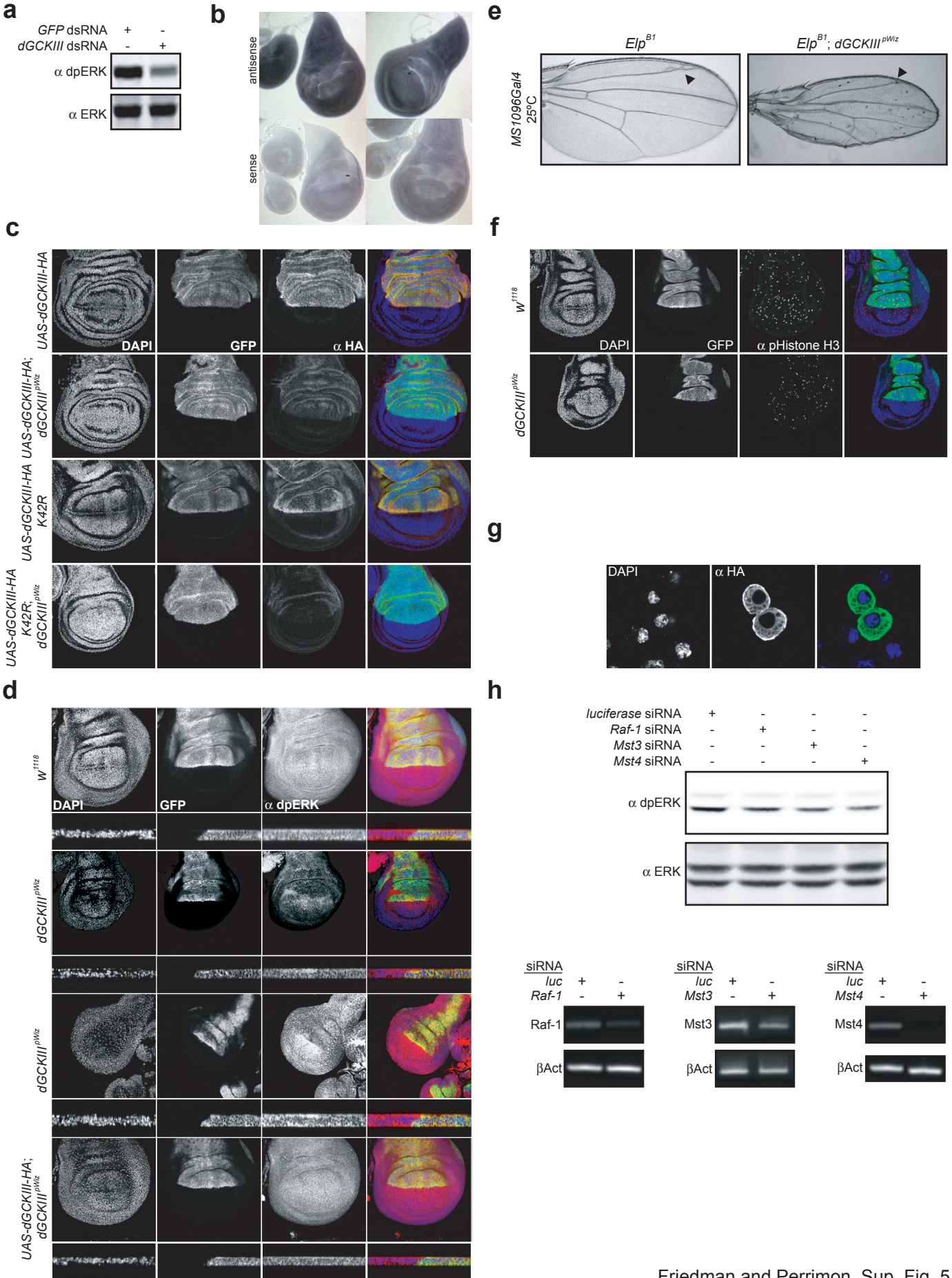
a**b****c****d****e**

Supplementary Figure 2 | Primary RTK/ERK Screen Results. **a**, Hierarchical clustering of all primary screen hits (see Sup. Table 1 for complete data and amplicon identifiers to retrieve sequences). Note that many genes exhibit dynamic regulation of ERK signaling, depending on stimulus state. The raw primary screen hit list, except for those 331 genes listed in the text, are non-validated and any given gene should be re-tested with multiple amplicons. **b**, Western blotting of dpERK elevation following insulin stimulus in ERK-YFP/CFP-MEK expressing primary screening S2R+ cells (see Methods). Compare to Sup. Fig. 2b showing similar activation. **c**, Score of each amplicon screened, at baseline and under insulin stimulus; each data point is an average of two replicates. Although similar numbers of negative regulators ($Z > 1.5$) were uncovered under both conditions, more positive regulators ($Z < -1.5$) were observed under insulin stimulation, a significant difference in amplicon score distribution ($p < 2.8 \times 10^{-20}$ by Kolmogorov-Smirnov test). **d**, We isolated all of the known core components of the RTK/ERK signaling pathway, indicated at left, a significant enrichment for pathway components ($p < 1.6 \times 10^{-14}$). As we raised the Z-score cutoff, we further enriched for known pathway components (right), indicating pathway components are preferentially isolated from the primary screen. Other genes previously characterized as regulators of RTK/ERK signaling were identified, including non-receptor tyrosine kinase src family member Src42D⁶⁵, the 14-3-3 proteins ϵ and ζ ⁶⁶, and PP2A/*mts*⁶⁷. **e**, Conservation of primary screen hits, by organism, determined from HomoloGene and InParanoid databases. p values for enrichment of each ortholog category were calculated using the hypergeometric distribution. For comparison, the ortholog conservation rate in the DRSC dsRNA collection, essentially the *Drosophila* genome, is 50%, 50%, 40%, and 21% for the human, mouse, worm, and yeast genomes, respectively.



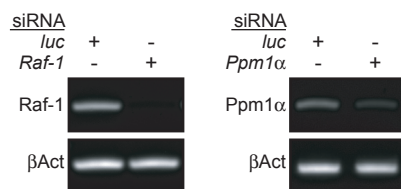
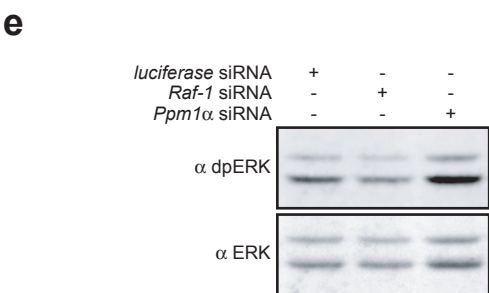
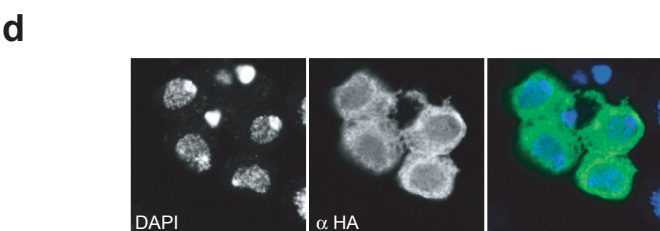
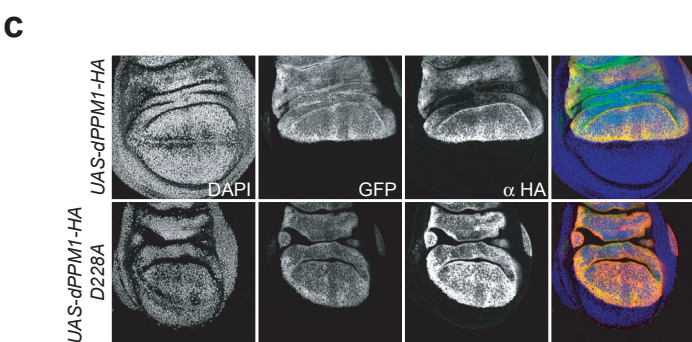
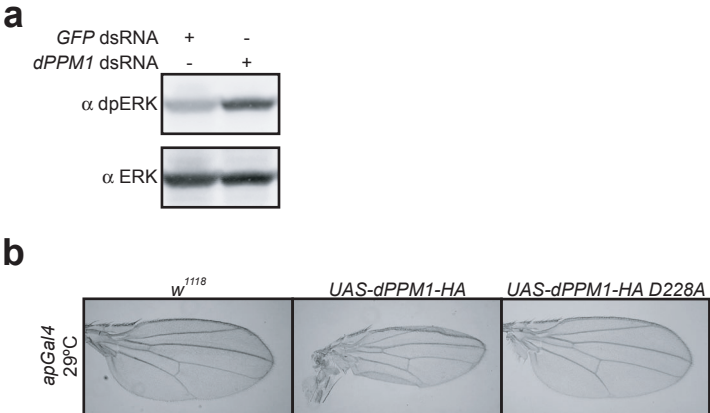
Supplementary Figure 3 | Secondary screen assay validation. **a**, Western blotting demonstrating activation of dpERK in Kc cells following insulin stimulus. A similar 10 minute peak activation was seen; these cells also have a secondary peak at 60 minutes. **b**, S2R+ cells stably expressing DER under metallothionein promoter were stimulated with conditioned media containing secreted Spitz/EGF⁵¹. A robust dpERK activation was seen after 10 minutes (“+ Spitz” in upper section and see dynamics in lower section). This activation was DER-dependent, as DER knockdown eliminated dpERK elevation. **c**, Kc cells stably expressing DER under metallothionein promoter were stimulated similarly for 10 minutes with sSpi-containing medium, demonstrating robust, DER-dependent ERK activation. **d**, Wild-type S2R+ cells incubated with dsRNAs targeting known pathway components had expected alterations in dpERK levels detected in our secondary screening assay, which normalized dpERK staining to total ERK antibody. Similar results were seen in wild-type Kc cells (not shown). **e**, S2R+mtDER cells at baseline or under sSpi stimulus also displayed expected effects of known pathway components on ERK activation. Similar results were seen in KcmtDER cells in the secondary assays. **f**, Compared to S2R+ cells given serum-free medium, S2R+ cells bathed in serum-free medium conditioned from growth in Kc cells demonstrated elevation of dpERK after 10 minutes. Knockdown of Pvf1 or Pvf2 in the Kc cells reduced this elevation, suggesting Kc cells secrete Pvfs which hyper-stimulate S2R+ cells through PVR activation. * $p < 0.05$ by Student’s *t* test.

Supplementary Figure 4 | Additional secondary screen results. **a**, Hierarchical clustering of secondary screens, as in Fig. 2a, with gene names. See Sup. Table 5 for complete data and amplicon identifiers. **b**, JNK pathway component knockdown in S2R+ cells at baseline. *D-jun* (*Jra*) and *D-fos* (*kay*) both negatively regulated dpERK levels, while JNK negative regulators *raw* and *puckered* were required for maximal ERK activation. **c**, Akt pathway component knockdown in Kc cells under insulin stimulus. Akt pathway components consistently reflected negative regulation of ERK activation, with positive components of the Akt pathway (*Chico*, *PDK1*, *Akt*, *Rheb*, *Raptor*, *Tor*, and *S6K*) inhibiting ERK activation, and negative components of the Akt pathway (*PTEN* and *Tsc2*) potentiating ERK activation. Note InR is positively required for both pathways. As the Akt pathway in general had little effect on ERK signaling under EGF stimulus (Fig. 2b), determining the *in vivo* role of the interaction of these pathways may require analysis in tissues free of EGFR activity, excluding, for example, imaginal discs.



Supplementary Figure 5 | Additional supporting data for dGCKIII. **a**, Western blotting of S2R+ cells following *dGCKIII* knockdown in insulin-simulated cells. Quantification of this result showed ~19% reduction in normalized dpERK signal intensity (n=5). Reduction in dpERK signal is consistent with our observations in the primary and secondary screens. Three additional amplicons targeting *dGCKIII* gave similar results in these and other dpERK assays. **b**, *In situ* hybridization detecting ubiquitous *dGCKIII* transcripts in third-instar wing imaginal discs. Two examples are shown of antisense- and control sense-probed discs, processed under identical conditions. BDGP microarray data suggests continuous expression of dGCKIII throughout *Drosophila* embryogenesis⁵⁴. Staining in eye discs showed a similar ubiquitous expression. **c**, Relative *apGal4*-directed expression of dGCKIII-HA and dGCKIII-HA K42R in wing imaginal discs visualized by anti-HA staining. *apGal4* dorsal compartment is marked by mCD8-GFP. Composite color images are at right. Both constructs appeared to be expressed at similar levels in wing discs, and similarly could be knocked down by co-expression of the *dGCKIII* hairpin. All discs were dissected and stained simultaneously, and imaging parameters were constant. Note little change in the GFP marker staining, indicating that transgene effects are not likely due to Gal4 titration. **d**, dpERK staining of early third instar wing discs expressing *dGCKIII* hairpin alone or with *dGCKIII* cDNA. Suppression of dpERK levels in the dorsal compartment, more apparent in z-sections, was consistent. Two examples of this suppression are shown. **e**, Suppression of *Elp^{BI}* ectopic wing vein phenotype with the *dGCKIII* hairpin. **f**, Cell proliferation, as measured by phospho-Histone H3 (pHH3) staining, in wing discs expressing the *dGCKIII* hairpin. We did not observe any decrease in pHH3 staining in the dorsal compartment or control *apGal4*, *UAS-GFP* discs. **g**, Immunofluorescent staining of dGCKIII-HA expressed in S2R+ cells indicating a significant proportion of protein localized at the plasma membrane. This localization does not appear to change with insulin stimulus or Raf overexpression (data not shown). **h**, Western blotting of dpERK in DU145 human prostate cancer cells following knockdown of *Raf-1*, *Mst3*, and *Mst4* with 100nM siRNAs. Although there is conflicting evidence for roles of Mst3 and 4 in regulation of ERK signaling⁵⁵⁻⁵⁸, no study thus far has analyzed Mst3/4 activity by loss-of-function assays. Results are shown following overnight starvation in serum-free medium. Quantification of this change showed ~20% and ~10% average reduction (n=3) in dpERK2 signal intensity normalized to total ERK2 for Mst3 and 4, respectively, comparable to the results with *dGCKIII* RNAi in S2R+ cells. RT-PCR results,

below, demonstrate reduction in indicated transcript abundance compared to β -actin control in DU145 cells. All reactions were within the linear range of amplification. GAPDH controls gave similar results as β -actin (not shown).



Supplementary Figure 6 | Additional supporting data for dPPM1. **a**, Western blotting of dpERK in S2R+ cells after insulin stimulus following dsRNA knockdown of *dPPM1*; an additional amplicon targeting this gene gave similar results. Quantification of this result showed a 28% increase in normalized dpERK signal intensity (n=9). **b**, Overexpression of dPPM1 but not the D228A mutant in the wing imaginal disc resulted in smaller wings, with significant upward curling, suggesting reduced tissue in the dorsal compartment, where *apGal4* is expressed. Ubiquitous, zygotic overexpression of dPPM1 was embryonic lethal at 29°C. **c**, Relative *apGal4*-directed expression of dPPM1-HA and dPPM1-HA D228A in wing imaginal discs visualized by anti-HA staining. *apGal4* dorsal compartment is marked by UAS-mCD8-GFP. Both constructs appeared to be expressed at similar levels in wing discs. All discs were dissected and stained simultaneously and imaging parameters were constant. Note we see little consistent change in the GFP marker staining, indicating that transgene effects are not likely due to Gal4 titration. **d**, Immunofluorescent staining of S2R+ cells expressing dPPM1-HA, showing general cytoplasmic staining of the tagged phosphatase. **e**, siRNA knockdown of *Raf-1* and *Ppm1α* in LNCaP prostate cancer cells, following overnight starvation and stimulation with 100ng/mL EGF for 10 minutes; 50nM siRNA was used for this experiment. Quantification of this result showed 44% reduction in normalized dpERK by *Raf-1* siRNA and 53% increase in normalized dpERK2 by *Ppm1α* siRNA (n=5). RT-PCR results, below, demonstrate reduction in indicated transcript abundance compared to β-actin control in LNCaP cells. All reactions were within the linear range of amplification. GAPDH controls gave similar results as β-actin (not shown).

Supplementary Notes

31. Boutros, M. et al. Genome-wide RNAi analysis of growth and viability in *Drosophila* cells. *Science* 303, 832-5 (2004).
32. Hild, M. et al. An integrated gene annotation and transcriptional profiling approach towards the full gene content of the *Drosophila* genome. *Genome Biol* 5, R3 (2003).
33. *Drosophila* RNAi Screening Center, www.flyrnai.org (2006).
34. Yanagawa, S., Lee, J. S. & Ishimoto, A. Identification and characterization of a novel line of *Drosophila* Schneider S2 cells that respond to wingless signaling. *J Biol Chem* 273, 32353-9 (1998).
35. Kiger, A. et al. A functional genomic analysis of cell morphology using RNA interference. *J Biol* 2, 27 (2003).
36. Clemens, J. C. et al. Use of double-stranded RNA interference in *Drosophila* cell lines to dissect signal transduction pathways. *Proc Natl Acad Sci U S A* 97, 6499-503 (2000).
37. Gabay, L., Seger, R. & Shilo, B. Z. In situ activation pattern of *Drosophila* EGF receptor pathway during development. *Science* 277, 1103-6 (1997).
38. Malo, N., Hanley, J. A., Cerquozzi, S., Pelletier, J. & Nadon, R. Statistical practice in high-throughput screening data analysis. *Nat Biotechnol* 24, 167-75 (2006).
39. Kulkarni, M. et al. Evidence of off-target effects associated with the use of long dsRNAs in *Drosophila* cell-based assays. *Nat Methods* in press (2006).
40. Stolc, V. et al. A gene expression map for the euchromatic genome of *Drosophila melanogaster*. *Science* 306, 655-60 (2004).
41. FlyBase, <http://www.flybase.org> (2006).
42. HomoloGene, <http://www.ncbi.nlm.nih.gov/entrez/query.fcgi?db=homologene> (2006).
43. InParanoid, <http://inparanoid.cgb.ki.se/> (2006).
44. Ensembl, <http://www.ensembl.org/> (2005).
45. Homophila, <http://superfly.ucsd.edu/homophila/> (2004).
46. Hong, P. & Wong, W. H. GeneNotes--a novel information management software for biologists. *BMC Bioinformatics* 6, 20 (2005).
47. Benjamini, Y. & Yekutieli, D. Quantitative trait Loci analysis using the false discovery rate. *Genetics* 171, 783-90 (2005).

48. Benjamini, Y., Drai, D., Elmer, G., Kafkafi, N. & Golani, I. Controlling the false discovery rate in behavior genetics research. *Behav Brain Res* 125, 279-84 (2001).
49. Ma, Y., Creanga, A., Lum, L. & Beachy, P. Prevalence of off-target effects in *Drosophila* RNAi screens. *Nature* in press (2006).
50. Neal, S. J., Gibson, M. L., So, A. K. & Westwood, J. T. Construction of a cDNA-based microarray for *Drosophila melanogaster*: a comparison of gene transcription profiles from SL2 and Kc167 cells. *Genome* 46, 879-92 (2003).
51. Schweitzer, R., Shaharabany, M., Seger, R. & Shilo, B. Z. Secreted Spitz triggers the DER signaling pathway and is a limiting component in embryonic ventral ectoderm determination. *Genes Dev* 9, 1518-29 (1995).
52. Duchek, P., Somogyi, K., Jekely, G., Beccari, S. & Rorth, P. Guidance of cell migration by the *Drosophila* PDGF/VEGF receptor. *Cell* 107, 17-26 (2001).
53. Roy, F., Laberge, G., Douziech, M., Ferland-McCollough, D. & Therrien, M. KSR is a scaffold required for activation of the ERK/MAPK module. *Genes Dev* 16, 427-38 (2002).
54. Berkeley *Drosophila* Genome Project, <http://www.bdgp.org/> (2006).
55. Schinkmann, K. & Blenis, J. Cloning and characterization of a human STE20-like protein kinase with unusual cofactor requirements. *J Biol Chem* 272, 28695-703 (1997).
56. Zhou, T. H. et al. Identification of a human brain-specific isoform of mammalian STE20-like kinase 3 that is regulated by cAMP-dependent protein kinase. *J Biol Chem* 275, 2513-9 (2000).
57. Dan, I. et al. Cloning of MASK, a novel member of the mammalian germinal center kinase III subfamily, with apoptosis-inducing properties. *J Biol Chem* 277, 5929-39 (2002).
58. Qian, Z., Lin, C., Espinosa, R., LeBeau, M. & Rosner, M. R. Cloning and characterization of MST4, a novel Ste20-like kinase. *J Biol Chem* 276, 22439-45 (2001).
59. Ofek, P., Ben-Meir, D., Kariv-Inbal, Z., Oren, M. & Lavi, S. Cell cycle regulation and p53 activation by protein phosphatase 2C alpha. *J Biol Chem* 278, 14299-305 (2003).
60. Cheng, A., Ross, K. E., Kaldis, P. & Solomon, M. J. Dephosphorylation of cyclin-dependent kinases by type 2C protein phosphatases. *Genes Dev* 13, 2946-57 (1999).

61. Lee, Y. S. & Carthew, R. W. Making a better RNAi vector for *Drosophila*: use of intron spacers. *Methods* 30, 322-9 (2003).
62. Pearson, G. et al. Mitogen-activated protein (MAP) kinase pathways: regulation and physiological functions. *Endocr Rev* 22, 153-83 (2001).
63. Roux, P. P. & Blenis, J. ERK and p38 MAPK-activated protein kinases: a family of protein kinases with diverse biological functions. *Microbiol Mol Biol Rev* 68, 320-44 (2004).
64. Yang, S. H., Sharrocks, A. D. & Whitmarsh, A. J. Transcriptional regulation by the MAP kinase signaling cascades. *Gene* 320, 3-21 (2003).
65. Laberge, G., Douziech, M. & Therrien, M. Src42 binding activity regulates *Drosophila* RAF by a novel CNK-dependent derepression mechanism. *Embo J* 24, 487-98 (2005).
66. Chang, H. C. & Rubin, G. M. 14-3-3 epsilon positively regulates Ras-mediated signaling in *Drosophila*. *Genes Dev* 11, 1132-9 (1997).
67. Ory, S., Zhou, M., Conrads, T. P., Veenstra, T. D. & Morrison, D. K. Protein phosphatase 2A positively regulates Ras signaling by dephosphorylating KSR1 and Raf-1 on critical 14-3-3 binding sites. *Curr Biol* 13, 1356-64 (2003).

Supplementary Table 2: Primary Screen hits by Gene Ontology Term Enrichment

GO ID	GO Term (Biological Process)	p value
9653	Morphogenesis	1.2E-14
8152	Metabolism	1.2E-13
8283	Cell proliferation	4.6E-13
9887	Organogenesis	5.8E-13
7049	Cell cycle	2.0E-12
6412	Protein biosynthesis	2.4E-12
7444	Imaginal disc development	5.5E-12
48477	Oogenesis	1.5E-11
6367	Transcription initiation (Pol II)	4.1E-11
7276	Gametogenesis	1.2E-10
8380	RNA splicing	2.6E-08
7067	Mitosis	5.9E-08
1654	Eye morphogenesis	1.1E-07
6355	Regulation of transcription	5.1E-07
30036	Actin cytoskeleton	1.3E-06
7399	Neurogenesis	3.6E-06
226	Microtubule cytoskeleton	4.6E-06
7422	Peripheral nervous system development	6.9E-06
30097	Hemopoiesis	7.6E-06
16477	Cell migration	1.2E-05
42981	Apoptosis	5.9E-04

GO ID	GO Term (Molecular Function)	p value
3735	Structural constituent of ribosome	4.0E-13
16251	General RNA Pol II transcription factor	2.1E-12
3723	RNA binding	4.5E-12
30528	Transcription regulator	2.7E-10
8248	Pre-mRNA splicing factor	5.3E-09
45182	Translation regulator	1.2E-05
3743	Translation initiation factor	1.8E-05
5525	GTP binding	5.0E-04
19887	Protein kinase regulator	7.7E-04

GO term enrichment calculated using GeneNotes software:

Hong, P. & Wong, W. H. GeneNotes--a novel information management software for biologists. *BMC Bioinformatics* 6, 20 (2005).

Supplementary Table 3: Overlapping hits from RTK/ERK and Morphology RNAi screens

Gene Symbol	Gene Name	FlyBase ID	Avg Baseline Z-score	Avg Insulin Z-score	Kc cells						S2R+ cells											
					A	M	D	S	Z	N	V	A	M	D	S	Z	N	V				
Akt1	Akt1	FBgn0010379	1.1	2.7																		
Arc-p34	Arc-p34	FBgn0032859	-1.3	-1.6																		
cact	cactus	FBgn0000250	-1.5	-2.4																		
cdc2	cdc2	FBgn00004106	-2.7	-2.6																		
Cdc27	Cdc27	FBgn0012058	3.1	-4.1																		
Cdk4	Cyclin-dependent kinase 4	FBgn0016131	-1.9	-2.7																		
Cdk9	Cyclin-dependent kinase 9	FBgn0019949	-0.5	4.9																		
CG13503	CG13503	FBgn0034695	0.5	-1.5																		
CG14217	CG14217	FBgn0031030	1.1	-2.1																		
CG5169	CG5169	FBgn0038477	0.9	-2.0																		
CG8878	BcDNA-LD23371	FBgn0027504	-0.8	-1.9																		
CycE	Cyclin E	FBgn0010382	-4.7	-5.9																		
CycT	Cyclin T	FBgn0025455	0.0	4.1																		
dco	discs overgrown	FBgn0002413	2.0	1.0																		
Dp	DP transcription factor	FBgn0011763	-3.8	-2.9																		
drk	downstream of receptor kinase	FBgn0004638	-1.8	-4.7																		
Dsor1	Downstream of raf1	FBgn0010269	-1.7	-1.2																		
ena	enabled	FBgn0000578	0.6	-2.1																		
Fs(2)Ket	Female sterile (2) Ketel	FBgn0000986	-2.4	-3.6																		
fwd	four wheel drive	FBgn0004373	1.8	1.9																		
fzy	fizzy	FBgn0001086	-0.8	-4.0																		
gig	gigas	FBgn0005198	0.4	-1.8																		
His3_3A	Histone H3.3A	FBgn0014857	-1.3	-4.6																		
Hsp83	Heat shock protein 83	FBgn0001233	0.7	1.8																		
if	inflated	FBgn0001250	-2.7	-1.1																		
Klp61F	Kinesin-like protein at 61F	FBgn0004378	1.7	-2.3																		
ksr	kinase suppressor of ras	FBgn0015402	-1.5	-7.0																		
mts	microtubule star	FBgn0004177	0.9	-3.4																		
Pak3	Pak3	FBgn0044826	0.5	-2.5																		
pav	pavarotti	FBgn0011692	2.4	-0.3																		
Pten	Pten	FBgn0026379	0.1	-2.7																		
puc	puckered	FBgn0004210	0.1	-3.9																		
Pvr	PDGF- and VEGF-receptor related	FBgn0032006	-3.8	-8.4																		
Rac2	Rac2	FBgn0014011	-0.1	-2.5																		
ran	ran	FBgn0020255	-1.6	0.1																		
Ras85D	Ras oncogene at 85D	FBgn0003205	-2.1	-5.9																		
Rho1	Rho1	FBgn0014020	-1.1	-1.9																		
RhoL	rho-like	FBgn0014380	-0.3	-2.1																		
S6k	RPS6-p70-protein kinase	FBgn0015806	-1.5	2.5																		
Sos	Son of sevenless	FBgn0001965	-2.9	-6.5																		
th	thread	FBgn0003691	-0.4	-6.2																		

Morphology data from Kiger, et al., 2003

- F-ACTIN**
- A variable, undefined
 - reduced, non-cortical
 - ~ fibers
 - + puncta, dots
 - o accumulated
 - < polarized
 - X processes, ruffles
- MICROTUBULE**
- M variable, undefined
 - reduced
 - + dots
 - <> aberrant or frequent mitotic spindles
 - | accumulated
 - | bipolar extensions or spikes
 - X processes
 - O disorganized, uniform
- DNA**
- D variable, undefined
 - small, condensed
 - + big, diffuse
 - ** multinucleated
- CELL SHAPE**
- S variable, undefined
 - flat
 - retracted
 - X processes, spiky, stretchy
 - | bipolar
 - O round, non-adherent
- CELL SIZE**
- Z variable, undefined
 - small
 - + big
- CELL NUMBER**
- N variable, undefined
 - O sparse
- CELL VIABILITY**
- V variable, undefined
 - † death

Reference:

Kiger, A. et al. A functional genomic analysis of cell morphology using RNA interference. *J Biol* 2, 27 (2003).

spr1	sprint																				Signaling		
Grp1	General receptor for phosphoinositides 1																				GAP/GEF/GTPase		
trio																					GAP/GEF/GTPase		
loner																					GAP/GEF/GTPase		
Rab11	Rab-protein 11																				GAP/GEF/GTPase		
CG18646																					GAP/GEF/GTPase		
rab3-GEF																					GAP/GEF/GTPase		
ran																					GAP/GEF/GTPase		
CG10628																					GAP/GEF/GTPase		
Epac																					GAP/GEF/GTPase		
Gtp-bp	GTP-binding protein																				GAP/GEF/GTPase		
Cell Cycle																							
CycE	Cyclin E																				Cell Cycle		
Rca1	Regulator of cyclin A1																				Cell Cycle		
cdc2	cdc2																				Cell Cycle		
fzy	fizzy																				Cell Cycle		
I(2)03709																					Cell Cycle		
Cdk4	Cyclin-dependent kinase 4																				Cell Cycle		
Cdc27																					Cell Cycle		
CycA	Cyclin A																				Cell Cycle		
CycT	Cyclin T																				Cell Cycle		
CG7597																					Cell Cycle		
CycG	Cyclin G																				Cell Cycle		
CycD	Cyclin D																				Cell Cycle		
Transcription Factor																							
CG31666																					Transcription Factor		
CG6686																					Transcription Factor		
crp	cropped																				Transcription Factor		
CG10955																					Transcription Factor		
I(2)NC136																					Transcription Factor		
Adf1	Adh transcription factor 1																				Transcription Factor		
Dp	DP transcription factor																				Transcription Factor		
CG6854																					Transcription Factor		
CG32133																					Transcription Factor		
h	hairy																				Transcription Factor		
CG14711, CG6808																					Transcription Factor		
E2f	E2F transcription factor																				Transcription Factor		
fru	fruitless																				Transcription Factor		
zfh1	Zn finger homeodomain 1																				Transcription Factor		
toy	twin of eyeless																				Transcription Factor		
Smox	Smad on X																				Transcription Factor		
vnd	ventral nervous system defective																				Transcription Factor		
Myb	Myb oncogene-like																				Transcription Factor		
CG1379																					Transcription Factor		
B-H1	BarH1																				Transcription Factor		
D19A																					Transcription Factor		
Chromatin/General TF																							
His3.3A	Histone H3.3A																				Chromatin		
E(Pc)	Enhancer of Polycomb																				Chromatin		
Cap-G																					Chromatin		
CG6701																					Chromatin		
dup	double parked																				Chromatin		
Mi-2																					Chromatin		
Caf1	Chromatin assembly factor 1 subunit																				Chromatin		
His4r	Histone H4 replacement																				Chromatin		
Spt6																					Chromatin		
His2A:CG31618																					Chromatin		
His3:CG31613																					Chromatin		
His4:CG31611																					Chromatin		
glu	gluon																				Chromatin		
kis	kismet																				Chromatin		
RpII33	RNA polymerase II 33kD subunit																				General TF		
TfIIIB	Transcription factor IIB																				General TF		
Rpb5																					General TF		
Sin3A																					General TF		
Trap36																					General TF		
brm	brahma																				General TF		
TfIIAlpha	Transcription factor IIFalpha																				General TF		
Rpb10																					General TF		
Med7																					General TF		
Trap80																					General TF		
Cytoskeletal																							
Act42A	Actin 42A																				Cytoskeletal		
shot	short stop																				Cytoskeletal		
Bap55	Brahma associated protein 55kD																				Cytoskeletal		
Klp61F	Kinesin-like protein at 61F																				Cytoskeletal		
Gl	Glued																				Cytoskeletal		
alphaTub84B	alpha-Tubulin at 84B																				Cytoskeletal		
alphaTub85E	alpha-Tubulin at 85E																				Cytoskeletal		
Act5C	Actin 5C																				Cytoskeletal		
CG1571																					Cytoskeletal		
ctp	cut up																				Cytoskeletal		
fill	flightless I																				Cytoskeletal		
Grip84	gamma-tubulin ring protein 84																				Cytoskeletal		
Metabolic/Enzyme																							
CG2964																					Metabolism		
CG9468																					Metabolism		
CG11198																					Metabolism		
CG1814																					Metabolism		
CG6984																					Metabolism		
GlcAT-P																					Metabolism		
CG10168																					Metabolism		
CG5844																					Metabolism		
mnd	minidiscs																				Metabolism		
CG33138																					Metabolism		


I(2)44DEa																					Metabolism		
rho	rhomboid																				Enzyme		
CG31146																					Enzyme		
egh	egghead																				Enzyme		
Ect3																					Enzyme		
RNA Processing/Translation																							
RpL7	Ribosomal protein L7																				Ribosome		
RpS26	Ribosomal protein S26																				Ribosome		
aret	arrest																				RNA Processing		
Smg5																					RNA Processing		
AGO1	Argonaute 1																				RNA Processing		
CG1884																					RNA Processing		
pAbp	polyA-binding protein																				RNA Processing		
CG13298																					RNA Processing		
qkr58E-1	quaking related 58E-1																				RNA Processing		
Hel25E	Helicase at 25E																				Splicing		
CG7757																					Splicing		
CG5454																					Splicing		
CG11146																					Signaling		
dock	dreadlocks																				Signaling		
ImpE3	Ecdysone-inducible gene E3																				Signaling		
Nplp3	Neuropeptide-like precursor 3																				Signaling		
Pvf3	PDGF- and VEGF-related factor 3																				Signaling		
eIF3-S10																					Translation		
eIF-1A	Eukaryotic initiation factor 1A																				Translation		
Ubiquitylation/Proteasomal																							
CG30382, Prosalpha6	Proteasome alpha6 subunit																				Proteasome		
Rpt1																					Proteasome		
CG2508																					Ubiquitylation		
CG30421																					Ubiquitylation		
ago	archipelago																				Ubiquitylation		
CG5505																					Ubiquitylation		
th	thread																				Ubiquitylation		
CG11700																					Ubiquitylation		
Receptor/Ion Transport																							
CG31645																					Receptor		
dsf	dissatisfaction																				Receptor		
Gr58c	Gustatory receptor 58c																				Receptor		
CG16801																					Receptor		
TyrR	Tyramine receptor																				Receptor		
CG7918																					Receptor		
DopR	Dopamine receptor																				Receptor		
svp	seven up																				Receptor		
btl	breathless																				Receptor		
CCKLR-17D3	CCK-like receptor at 17D3																				Receptor		
Gr21a	Gustatory receptor 21a																				Receptor		
Gr2a	Gustatory receptor 2a																				Receptor		
mAcR-60C	muscarinic Acetylcholine Receptor 60C																				Receptor		
robo3																					Receptor		
hoe1	hoepel1																				Ion Transport		
CG12602																					Ion Transport		
nrv1	nervana 1																				Ion Transport		
SerT	Serotonin transporter																				Ion Transport		
CG4357																					Ion Transport		
nAcRalpha-96Aa	nicotinic Acetylcholine Receptor alpha 96Aa																				Ion Transport		
CG6608																					Ion Transport		
Hk	Hyperkinetic																				Ion Transport		
cngl	CNG channel-like																				Ion Transport		
CG15094																					Ion Transport		
Other																							
CG9455																					Other		
spas	spastin																				Other		
CG6842																					Other		
Fs(2)Ket	Female sterile (2) Ketel																				Protein Transport		
Karybeta3	Karyopherin beta 3																				Protein Transport		
Syx5	Syntaxin 5																				Trafficking		
beta'Cop	beta'-coatomer protein																				Trafficking		
alphaCop	alpha-coatomer protein																				Trafficking		
deltaCOP	delta-coatomer protein																				Trafficking		
Bap	Beta Adaptin																				Trafficking		
betaCop	beta-coatomer protein																				Trafficking		
Unknown Function																							
CG31814																					Unknown		
CG11990																					Unknown		
CG32791																					Unknown		
CG3332																					Unknown		
CG6550																					Unknown		
defl	deflated																				Unknown		
CG5546																					Unknown		
CG5830																					Unknown		
CG31302																					Unknown		
CG9667																					Unknown		
CG32679																					Unknown		
twit	twilight																				Unknown		
CG3878																					Unknown		
CG6907																					Unknown		
CG30476																					Unknown		
CG8963																					Unknown		
CG14447	Glutamate receptor binding protein																				Unknown		
CG13784																					Unknown		
CG11416																					Unknown		
CG1841																					Unknown		
CG13779																					Unknown		
side	sidestep																				Unknown		
B4																					Unknown		


CG11451																						Unknown	
CG12155																						Unknown	
CG12452																						Unknown	
CG13819																						Unknown	
CG14119																						Unknown	
CG14342																						Unknown	
CG14420																						Unknown	
CG14952																						Unknown	
CG15060																						Unknown	
CG15321																						Unknown	
CG16969																						Unknown	
CG17665																						Unknown	
CG1908																						Unknown	
CG31705																						Unknown	
CG31763																						Unknown	
CG32771																						Unknown	
CG3563																						Unknown	
CG6770																						Unknown	
CG7282																						Unknown	
CG7552																						Unknown	
CG8108																						Unknown	
east	enhanced adult sensory threshold																					Unknown	
l(2)dtl	lethal-(2)-denticleless																					Unknown	
pxb																						Unknown	
raw	raw																					Unknown	
CG13320																						Unknown	
CG14213																						Unknown	
CG14400																						Unknown	
CG14460																						Unknown	
CG14512																						Unknown	
CG15311																						Unknown	
CG31788																						Unknown	
CG5172																						Unknown	
CG7556																						Unknown	
slam	slow as molasses																					Unknown	
yellow-d2																						Unknown	
CG40099																						Unknown	
No Annotation																							
HFA00956																						No annotation	
HFA01082																						No annotation	
HFA01091																						No annotation	
HFA01508																						No annotation	
HFA01639																						No annotation	
HFA01726																						No annotation	
HFA03655																						No annotation	
HFA04827																						No annotation	
HFA05237																						No annotation	
HFA05488																						No annotation	
HFA05595																						No annotation	
HFA05691																						No annotation	
HFA05715																						No annotation	
HFA05860																						No annotation	
HFA05861																						No annotation	
HFA07849																						No annotation	
HFA08092																						No annotation	
HFA08764																						No annotation	
HFA08786																						No annotation	
HFA08973																						No annotation	
HFA09077																						No annotation	
HFA09200																						No annotation	
HFA09359																						No annotation	
HFA10097																						No annotation	
HFA10152																						No annotation	
HFA12455																						No annotation	
HFA12829																						No annotation	
HFA14061																						No annotation	
HFA17488																						No annotation	
HFA18991																						No annotation	
HFA19091																						No annotation	
HFA20801																						No annotation	

Conservation calls are based strictly on InParanoid and Homologene ortholog queries (October 2004) and therefore may not reflect more detailed analyses.

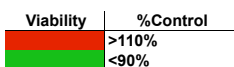
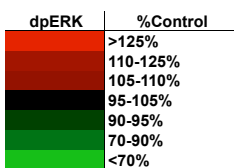
Annotation categories are manual groupings of Gene Ontology data queried from FlyBase (October 2004) and therefore may not reflect more comprehensive studies of function.

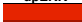






"Validated"



 indicates an additional ampicon targeting the given gene affected ERK activation in S2R+ cells at baseline or under insulin stimulation. See Methods for details.

 indicates an additional ampicon targeting the given gene did not affect ERK activation in S2R+ cells at baseline or under insulin stimulation. See Methods for details.

 indicates no additional ampicons targeting the given gene were tested



dpERK	%Control
	>125%
	110-125%
	105-110%
	95-105%
	90-95%
	70-90%
	<70%

Viability	%Control
	>110%
	<90%

Friedman and Perrimon
Supplementary Table 7: Validated regulators induced by RTK/ERK signaling *in vivo*

		Asha, et al., 2003 RasY12 Expression Dataset (Fold Induction)	Jordan, et al., 2005 EGFR Ovary Dataset*	MAPK Phenotype					Conservation				Human Disease	Annotation	ERKViability	Validated
				S2R+		Kc167		Human	Mouse	Worm	Yeast					
Gene	Protein			Baseline	Pvf Hyperstim	Insulin	sSpitz/EGF					sSpitz/EGF				
Act42A	Actin 42A	-0.98												Cytoskeletal		
Act5C	Actin 5C	-1.4												Cytoskeletal		
Adf1	Adh transcription factor 1	1.16												Transcription Factor		
aur	aurora	1.02												Kinase		
Axn	Axin	0.93												Signaling		
B4		0.75												Unknown		
Bap55	Brahma associated protein 55kD	0.69	GOFupLOFdown											Cytoskeletal		
Caf1	Chromatin assembly factor 1 subunit	1.68	GOFupLOFdown											Chromatin		
Cap-G		1.23	GOFupLOFdown											Chromatin		
cdc2	cdc2	2.97												Cell Cycle		
Cdk4	Cyclin-dependent kinase 4	1.24												Cell Cycle		
CG11198		1												Metabolism		
CG11451		2.98												Unknown		
CG12155		1.39												Unknown		
CG13298		1.12												RNA Processing		
CG13779		-1.03												Unknown		
CG13784		-1.33												Unknown		
CG14217		0.98												Kinase		
CG14512		1.16												Unknown		
CG16969		0.89												Unknown		
CG1841		0.82												Unknown		
CG1884			GOFupLOFNC											RNA Processing		
CG18854, IP3K1		-1.05												Kinase		
CG30421		1.37												Ubiquitylation		
CG31666		3.03												Transcription Factor		
CG3563			GOFupLOFdown											Unknown		
CG3878			GOFdownLOFup											Unknown		
CG6686		0.57	GOFdownLOFup											Transcription Factor		
CG6701		0.28												Chromatin		
CG6770		-1.2												Unknown		
CG6854		0.86												Transcription Factor		
CG6984			GOFdownLOFup											Metabolism		
CG8878		1.02												Kinase		
CG9455		0.74												Other		
CG9667		0.77												Unknown		
crp	cropped	1.82												Transcription Factor		
ctp	cut up	1.11												Cytoskeletal		
CycA	Cyclin A	1.52												Cell Cycle		
CycE	Cyclin E	2.77												Cell Cycle		
dock	dreadlocks	0.54												Signaling		
Dp	DP transcription factor	1.22	GOFupLOFdown											Transcription Factor		
Drk	downstream of receptor kinase (Grb2)		GOFupLOFdown											Signaling		
egh	egghead	0.63												Enzyme		
flw	flap wing	1.98												Phosphatase		
for	foraging	1.03	GOFupLOFdown											Kinase		
Fs(2)Ket	Female sterile (2) Ketel	0.66												Protein Transport		
fwd	four wheel drive	0.72												Kinase		
fzy	fizzy	2.79												Cell Cycle		
glu	gluon	2.25	GOFupLOFdown											Chromatin		
Gprk2	G protein-coupled receptor kinase 2	0.42												Kinase		
Grip84	gamma-tubulin ring protein 84	0.56												Cytoskeletal		
hoe1	hoepe1	-2.59												Ion Transport		
JIL-1		1.12												Kinase		
kis	kismet	0.93	GOFupLOFNC											Chromatin		
Klp61F	Kinesin-like protein at 61F	2.99												Cytoskeletal		
l(2)NC136		0.7	GOFupLOFdown											Transcription Factor		
mnd	minidiscs	1.08	GOFdownLOFup											Metabolism		
Myb	Myb oncogene-like	0.9												Transcription Factor		
nrv1	nervana 1	0.87												Ion Transport		
Pk61C	Protein kinase 61C	0.87												Kinase		
Pten		1.4												Phosphatase		
PTP-ER	Protein tyrosine phosphatase-ERK/Enhancer of Ras1	0.51												Phosphatase		
puc	puckered		GOFupLOFdown											Phosphatase		
qkr58E-1	quaking related 58E-1		GOFdownLOFup											RNA Processing		
Rac1		0.86												GAP/GEF/GTPase		
Rack1	Receptor of activated protein kinase C 1	-1.28												Signaling		
Ras85D	Ras oncogene at 85D	0.92												GAP/GEF/GTPase		
Rca1	Regulator of cyclin A1	0.63												Cell Cycle		
RhoGAP19D			GOFupLOFdown											GAP/GEF/GTPase		
RhoGAP71E		1.57												GAP/GEF/GTPase		
Rpb5		0.51												General TF		
RpL7	Ribosomal protein L7	-1.19												Ribosome		
RpS26	Ribosomal protein S26	-1.52												Ribosome		
shn	schnurri	0.93												Transcription Factor		
shot	short stop	1.02												Cytoskeletal		
Sin3A		1.99												General TF		
Smg5			GOFupLOFdown											RNA Processing		
Smox	Smad on X	1.07												Transcription Factor		
spas	spastin	0.73												Other		
Spt6		0.58												Chromatin		
Tak1	TGF-beta activated kinase 1	1.47												Kinase		
TfIIIB	Transcription factor IIB	1.51												General TF		



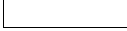
* "GOF": gain-of-function RTK/ERK pathway components; "LOF": loss-of-function RTK/ERK pathway components; "down"/"up": transcripts induced or repressed by GOF or LOF analysis; "NC": no change








References



Asha, H. et al. Analysis of Ras-induced overproliferation in *Drosophila* hemocytes. *Genetics* 163, 203-15 (2003).
 Jordan, K. C. et al. Genome wide analysis of transcript levels after perturbation of the EGFR pathway in the *Drosophila* ovary. *Dev Dyn* 232, 709-24 (2005).

Conservation calls are based strictly on InParanoid and Homologene ortholog queries (October 2004) and therefore may not reflect more detailed analyses.
 Annotation categories are manual groupings of Gene Ontology data queried from FlyBase (October 2004) and therefore may not reflect more comprehensive studies of function.

"Validated"

	indicates an additional amplicon targeting the given gene affected ERK activation in S2R+ cells at baseline or under insulin stimulation. See Methods for details.
	indicates an additional amplicon targeting the given gene did not affect ERK activation in S2R+ cells at baseline or under insulin stimulation. See Methods for details.
	indicates no additional amplicons targeting the given gene were tested

dpERK	%Control
	>125%
	110-125%
	105-110%
	95-105%
	90-95%
	70-90%
	<70%

Viability	%Control
	>110%
	<90%

Gene	S2 mtRas ^{V12}	
	Insulin	CuSO ₄ - Induced
14-3-3epsilon	Red	Green
14-3-3zeta	Red	Green
ago	Black	Green
alphaCop	Green	Dark Green
aur	Red	Dark Green
betaCop	Green	Dark Green
beta'Cop	Green	Dark Green
cdc2	Green	Dark Green
CG11198	Green	Dark Green
CG11416	Green	Dark Green
CG11451	Red	Dark Green
CG11700	Light Green	Light Green
CG15060	Green	Dark Green
CG1814	Green	Dark Green
CG18646	Green	Dark Green
CG2049	Black	Dark Green
CG30387	Green	Light Green
CG30476	Green	Dark Green
CG31302	Light Green	Dark Green
CG31763	Green	Dark Green
CG32183	Green	Dark Green
CG33138	Green	Dark Green
CG3563	Green	Dark Green
CG5172	Black	Dark Green
CG5546	Green	Dark Green
CG5844	Green	Dark Green
CG6550	Green	Dark Green
CG6686	Black	Dark Green
CG6701	Green	Dark Green
CG6842	Green	Dark Green
CG7282	Black	Dark Green
CG7757	Black	Dark Green
CG7918	Green	Dark Green
CG8878	Green	Dark Green
cnk	Green	Light Green
CycA	Green	Dark Green
CycE	Green	Dark Green
CycT	Red	Dark Green
deltaCOP	Green	Dark Green
Dp	Green	Dark Green
Dsor1	Green	Light Green
dup	Green	Dark Green
flw	Green	Dark Green
for	Black	Dark Green
fru	Light Green	Light Green
Fs(2)Ket	Green	Light Green
fzy	Light Green	Dark Green

Friedman and Perrimon

Supplementary Table 8: Genes which suppress Ras^{V12}-mediated ERK activation

Grp1		
h		
HFA01082		
HFA01091		
HFA05237		
HFA05715		
HFA08092		
HFA09077		
HFA09359		
HFA10152		
HFA17488		
His2A:CG31618		
His3:CG31613		
His4r		
Hk		
Klp61F		
ksr		
l(2)03709		
mRNA-capping-enzyme		
Pak3		
phl		
Pp1-13C		
Pp1-87B		
puc		
Rab11		
rab3-GEF		
ran		
Ras85D		
Rpb10		
Rpb5		
Rpll33		
RpL7		
Rpt1		
shn		
spri		
th		
Tie		
trio		

